Reprinted from ACS SYMPOSIUM SERIES, No. 263
RESONANCES IN ELECTRON-MOLECULE SCATTERING
VAN DER WAALS COMPLEXES, AND REACTIVE CHEMICAL
DYNAMICS
Donald G. Truhlar, Editor

Roles Played by Metastable States in Chemistry

JACK SIMONS

Department of Chemistry, University of Utah, Salt Lake City, UT 84112

Metastable states are important in chemistry for reasons which relate to the fact that such states have finite lifetimes and finite Heisenberg energy widths. They are observed in spectroscopy as peaks or resonances superimposed on the continua in which they are buried. Their fleeting existence provides time for energy transfer to occur between constituent species which eventually become separated fragments. It is often the rate of such intra-fragment energy transfer which determines the lifetimes of resonances. The theoretical exploration of metastable states presents special difficulties because they are not discrete bound states. However, much of the machinery which has proven so useful for stationary electronic and vibrational-rotational states of molecules has been extended to permit resonance energies and lifetimes to be evaluated. In this contribution, examples of electronic shape and Feshbach, rotational and vibrational predissociation, and unimolecular dissociation resonances will be examined. Finally, a novel situation will be treated in which the energy transfer dictating the decay rate of the metastable species involves vibration-to-electronic energy flow followed by electron ejection.

The purposes of this chapter are to provide overview and perspective concerning the various kinds of metastable species found in chemical systems as well as to focus attention on an interesting class of temporary anions (1-4) whose lifetimes are governed by vibration-electronic coupling strengths. To emphasize the importance of metastable states in experimental chemistry, it is useful to first analyze how they are created via collisional or photon absorption processes. This provides a basis for discussing the signatures which metastable states leave in the instrumental responses seen in the laboratory. Having introduced metastable states in relation to the experimental situations in which they arise, it is useful to

0097-6156/84/0263-0003$06.00/0

distinguish between two primary categories of such species and to classify many of the systems treated in this symposium. This overview and categorizing focuses attention on the properties (e.g., mass, angular momentum, energy, potential energy surfaces, internal energy distribution) which determine the decay rates or lifetimes of particular species.

After giving an overview and interpretative treatment of a wide variety of metastable systems, this paper treats in somewhat more detail a class of highly vibrationally excited molecular anions which undergo electron ejection at rates determined by the strength of vibration-electronic coupling present in the anion. The findings of theoretical simulations of the electron ejection process as well as the experimental relevance of such temporary anions are discussed.

Metastable states as they occur in collisions and half collisions.

One can form metastable states (denoted here by AB*) either by bringing together two fragments (A and B) in a collision experiment or by exciting a bound state of the AB system using, for example, photon absorption or electron impact excitation. In situations where bound-state excitation is employed, the subsequent decay of the metastable to produce fragments (A and B) is termed a "half collision". The decay rate or lifetime (τ) of the excited state can, in some cases, be inferred from the Heisenberg component to the width (Γ) of the measured resonance feature in the bound-state absorption or excitation spectrum. It is often very difficult to extract from the total observed linewidth the component due to the decay of the corresponding state. Unresolved rotational structure and Doppler broadening often dominate the linewidth. Only for lifetimes shorter than 10^{-9} s (or $\Gamma \sim 0.03$ cm^{-1}) is it likely that the Heisenberg width will be a major component. For very long lived states, the lifetime may be measured by monitoring the time evolution of the product fragment species, by, for example, laser induced fluorescence or the absorption spectrum of one of the fragments produced. If one or both of the fragments are ionic, ion detection methods can be used. The appearance of structure in the absorption spectrum superimposed upon a background continuum is a result of the strong-interaction region component of the resonance-state wavefunction. This is the component of the metastable specie's wavefunction in which the fragments A and B reside within the region where their interfragment potential energy is significant. For fragment separations outside this region, the term "asymptotic" is employed. It is this "in close" part of the wavefunction that characterizes resonances and that may carry strong oscillator strength from the underlying bound state. Since in the lower AB state the A--B relative motion is bound and hence localized, it is only the localized part of the excited-state wavefunction which will appreciably overlap the ground-state wavefunction. Hence for excited metastable states, which possess large valence-region components, the electric dipole transition matrix element can be substantial. In contrast, excitation from the lower bound state to nonresonant dissociative excited states gives rise to smaller transition dipoles, because such excited states have small valence-region components and hence weaker absorption intensities.

For experiments in which two fragments collide to produce metastable species which subsequently undergo decay, the lifetime of the metastable state is reflected in the kinetic energy dependence of the elastic, inelastic, and reactive cross-sections characterizing the collision events. Such experiments measure cross-sections as the initial relative kinetic energy of the fragments is scanned. They may also monitor the kinetic energy of one or both of the fragments ejected from the metastable species. Such cross-sections when plotted as functions of the fragment relative kinetic energy display resonance features in the vicinity of each metastable-state energy. Collisionally formed states are called metastable or resonances if their lifetimes are substantially longer than the "transit times" which one would calculate for the fragments based upon knowledge of their asymptotic relative kinetic energies. The simple fact that the fragments remain in close contact longer than expected based on their transit time is what allows interfragment energy transfer to be so efficient in metastable species. Given interaction times of the order of $10\text{-}10^{13}$ times the transit time, [a typical transit time for molecules colliding at room temperature is $\sim 10^{-13}$ s], even small rates of energy transfer per interfragment vibration can result in large net energy transfers during the state's lifetime. Such enhanced efficiency for energy transfer results in higher probabilities that the product fragments exit in different internal states than were occupied in the initial collision pair. This is one of the most chemically important characteristics of metastable states.

Two Principle Categories of Resonance States. Denoting the internal energies of the separated fragments (A and B) by $E_{Ai} + E_{Bj}$, all metastable or resonance states can be subdivided into those whose total energy E_r lies either below or above each such asymptotic energy. As is shown below, this division is chemically meaningful because the physical features which determine the energies and lifetimes of the two types of resonances defined in this manner are different.

At energies above each $E_{Ai} + E_{Bj}$ one can expect to find orbiting resonances (also known as shape resonances) if the fragments experience an attractive potential (V) varying more strongly than r^{-2} and have non-zero relative angular momentum (ℓ). Here r represents the coordinate which asymptotically is the distance between the centers of mass of the two fragments. In elastic or inelastic collisions, the entering and exiting fragments have identical chemical composition but their internal (e.g., vibrational, rotational, electronic) states may differ. For reactive processes which proceed through a metastable state, the entering and exiting species are chemically different. The effective radial potentials $V + \hbar^2\ell(\ell+1)/2r^2\mu$ depicted in Figure (1) for various ℓ values may then support states whose total energy exceeds $E_{Ai} + E_{Bj}$ but which can decay only by the two fragments of relative reduced mass μ tunneling through the "angular momentum barrier" arising from the $\hbar^2\ell(\ell+1)/2\mu r^2$ factor in interfragment angular kinetic energy (i.e., the interfragment rotation). The tunneling lifetimes of these resonances are determined by the height and thickness of the angular barrier and the fragment reduced mass μ.

At energies below each fragment energy $E_{Ai} + E_{Bj}$, target-excited or Feshbach resonances are to be expected. Although these metastable states cannot decay to the $E_{Ai} + E_{Bj}$ asymptotic state, they possess enough energy to couple to the continua of lower fragment states (e.g., to $E_{Ai-1} + E_{Bj}$ or $E_{Ai} + E_{Bj-1}$; see Figure (2)). What makes these states metastable is the fact that not enough of their total energy is initially (i.e., as they are created) contained in the dissociative coordinate r. They have ample energy in the internal intrafragment degrees of freedom; however, some of this energy must be redistributed to the asymptotically dissociative motion before the resonance state can decay. The lifetimes of such target-excited states are determined by the strength of the coupling between the fragment internal degrees of freedom and the interfragment motion which, in turn, depends upon the curvature and anharmonicity of the system's potential energy surface. The position or energy E_r of the resonance state relative to its asymptotically closed reference energy $E_{Ai} + E_{Bj}$ is determined by the strength of the attractive potential between the A and B fragments in the E_{Ai} and E_{Bj} states; the stronger this attraction, the further below $E_{Ai} + E_{Bj}$ the Feshbach resonance should lie. A decay channel is said to be closed if the total energy of the system lies below the asymptotic energy of this channel. Thus metastable species can only decay to produce open-channel products. It is also possible to have target-excited resonances that lie above the $E_{Ai} + E_{Bj}$ asymptotic; these are discussed elsewhere (5).

Examples of Orbiting and Target-Excited Resonances

To better appreciate the chemical significance of both classes of metastable species it is helpful to examine several examples of such species. This overview is by no means intended to be exhaustive either with respect to the systems it covers or concerning references to workers in the area. Its purpose is to illustrate how metastable states can have important effects in chemical experiments. Therefore, the treatment given here is rather qualitative and directed toward the interested but non-expert reader.

Because electrons have much smaller mass than atomic nuclei, it is natural to distinguish between situations in which an electron is one of the fragment particles and those in which both fragments are so called heavy particles (i.e., atoms, molecules or ions). In the former case, the asymptotic fragment internal energies $E_{Ai} + E_{Bj}$ reduce to the energies of the atomic or molecular fragment since the electron fragment has no internal energy levels of its own (external magnetic field effects are ignored).

Electronic Shape Resonances. In the first three examples given below in Table I, the orbiting resonance can be viewed as forming when an electron of kinetic energy E_r enters an empty low-energy orbital of the atomic or molecular target fragment. As indicated in Table I, the active orbital has, in every case, nonzero angular momentum components which give rise to the barrier through which the electron must tunnel to escape. The attractive part of the

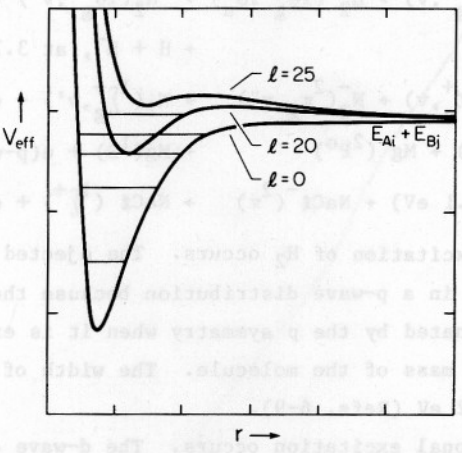

Figure 1: Effective potentials $V + \hbar^2 J(J(1)/2\mu r^2$ for $\ell = 0, 20, 25$.

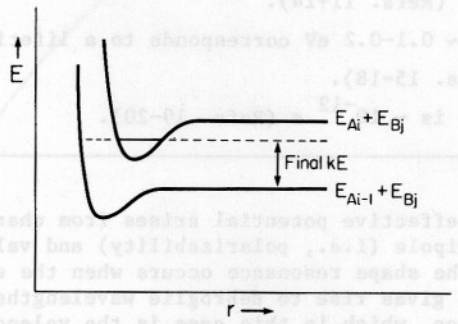

Figure 2: A Feshbach resonance exists below $E_{Ai} + E_{Bj}$ but above dissociation to $E_{Ai-1} + E_{Bj}$. The kinetic energy (KE) of the ejected A and B fragments is also shown.

Table I. Electronic Shape Resonance Examples

Formation Process	Decay Products
$e(3.7\ eV) + H_2(1\sigma_g^2, v) \rightarrow H_2^-(1\sigma_g^2 1\sigma_u)$	$\rightarrow H_2(1\sigma_g^2, v') + e(p\ wave)$[a]
	$\rightarrow H + H^-$, at 3.73 eV (Ref.10)
$e(2.3\ eV) + N_2\ (^1\Sigma_g^+, v) \rightarrow N_2^-(^2\pi_g, v'')$	$\rightarrow N_2(^1\Sigma_g^+, v') + e(d\text{-}wave)$[b]
$e(0.3\ eV) + Mg(^1S) \rightarrow Mg^-(^2P^o)$	$\rightarrow Mg(^1S) + e(p\text{-}wave)$[c]
$NaCl^-(^2\Sigma^+) + h\nu(2.1\ eV) \rightarrow NaCl^-(^2\pi)$	$\rightarrow NaCl\ (^1\Sigma^+) + e(p\text{-}wave)$[d]

a) Vibrational excitation of H_2 occurs. The ejected electron comes off primarily in a p-wave distribution because the $1\sigma_u$ orbital of H_2 is dominated by the p symmetry when it is expanded about the center of mass of the molecule. The width of this state is greater than 2 eV (Refs. 6-9).

b) Again vibrational excitation occurs. The d-wave character is dictated by the d-like symmetry of the active $1\pi_g$ antibonding orbital of N_2. The width $\Gamma \sim 0.6$ eV corresponds to a lifetime of $\sim 10^{-14}$ s (Refs. 11-14).

c) The width $\Gamma \sim 0.1\text{-}0.2$ eV corresponds to a lifetime of $2 - 4 \times 10^{-14}$ s (Refs. 15-18).

d) The lifetime is $\sim 10^{-12}$ s (Refs. 19-20).

electron-target effective potential arises from charge-dipole, charge-induced dipole (i.e., polarizability) and valence-level interactions. The shape resonance occurs when the energy of the ejected electron gives rise to deBroglie wavelengths in the strong-interaction region, which in this case is the valence region, that permit the electron's radial wavefunction to establish a standing wave pattern in the region between the two inner turning points of the effective potential (see Figure 1). In all of the examples illustrated here, only the ground electronic-state fragment is involved. Such does not have to be the case, however; orbiting resonances can arise from the binding of an electron with $\ell \neq 0$ to an excited electronic state of the fragment.

The relevance of the above kind of electronic shape resonance to chemistry is twofold. First, in environments such as plasmas, electrochemical cells, and the ionosphere, where free electrons are prevalent, the formation of such temporary anions can provide avenues for the free electrons to "cool down" by transferring kinetic energy to the internal (vibrational and/or electronic) degrees of freedom of the fragment. (6-14) Second, metastable states may play important roles in quenching excited electronic

states of atoms and molecules by providing a mechanism through which electronic energy can be transformed to fragment internal energy. For example, H_2^- ($1\sigma_g^2 1\sigma_u$) is invoked as an intermediate to explain the quenching of electronically excited (21-21) Na($3p;^2P^o$) and (23 Mg(^1P) by H_2 ($1\sigma_g^2$,v) to yield vibrationally hot H_2:

$$Na(^2P) + H_2(v) \rightarrow Na^+H_2^- \rightarrow Na(^1S) + H_2(1\sigma_g^2, v'),$$

$$Mg(^1P^o) + H_2(v) \rightarrow Mg^+(^2S)H_2^- \rightarrow Mg(^1S) + H_2(v').$$

In these examples, the metastable H_2^- does not actually undergo electron loss because the Na^+ or Mg^+ ion "retrieves" the electron as the complex dissociates leaving the H_2 vibrationally excited and the Na or Mg atom in its ground state. Recent work on electron transmission spectroscopy studies of unsaturated hydrocarbons (24) demonstrates that electronic shape resonances may be essentially ubiquitous in chemical systems which possess low-energy vacant orbitals and the availability of electron density to enter such orbitals.

Electronic Feshbach Resonances. In Table II are a few examples of target-excited or Feshbach resonances in which the ejected electron is initially attached to an electronically excited state of the fragment. Note that the angular properties (i.e., p-wave, s-wave, etc.) of the ejected electron are again constrained by the symmetries of the metastable state and the lower lying target state to which it decays. In the case of $H^-(2p^2, {}^3P^e)$, parity constraints even forbid direct ejection of a p-wave electron (odd parity) to leave the H atom in the H(1s,^{2}S) (even parity) ground state. $H^-(2p^2, {}^3P^e)$ must first radiate to produce the $H^-(2s2p, {}^3P^o)$ metastable state which can then undergo Feshbach decay to produce H(1s,^{2}S) and a p-wave electron. In contrast, the seemingly similar metastable $Na^-(3p^2, {}^3P^e)$ state of Na^- can undergo radiative decay to $Na^-(3s3p, {}^3P^o)$ and subsequent tunneling (not Feshbach) decay to Na (3s,^{2}S) and e(p-wave); direct Feshbach decay of $Na^-(3p^2, {}^3P^e)$ to Na(3s,^{2}S) and e(p-wave) is parity forbidden as was the case in H^-.

Electronic Feshbach resonances are often very long lived and hence have narrow (often < 0.01 eV) widths. Their lifetimes are determined by the coupling between the quasibound and asymptotic components of their electronic wavefunctions. Because the Feshbach decay process involves ejection of one electron and deexcitation of a second, it proceeds via the two-electron terms e^2/r_{ij} in the Hamiltonian. For example, the rate of electron loss in $H^-(2s2p, {}^3P^o)$ is proportional to the square of the two-electron integral $\langle 2s2p|e^2/r_{12}|1s\ kp\rangle$, where kp represents the continuum p-wave orbital. This integral, and hence the decay rate, is often quite small because of the size difference between the 2s or 2p and 1s orbitals and because of the oscillatory nature of the kp orbital. In fact, series of Feshbach resonances involving, for example, nsnp → n's kp decay often show (29) lengthening lifetimes as functions of increasing n. This trend can be explained in terms of both the greater radial size difference and the increasing oscillatory character (due to increased kinetic energy of the ejected electron) of the kp orbital as n increases. Both trends tend to make the coupling integral $\langle nsnp|e^2/r_{12}|n'skp\rangle$ smaller.

Table II. Electronic Feshbach Resonance Examples

Metastable Species		Decay Product
$He^-(1s2s^2, {}^2S)$	→	$He(1s^2, {}^1S) + e(s\text{-wave})$[a]
$H^-(2p^2, {}^3P^e)$[b]	→	$H^-(2s2p, {}^3P^o) + h\nu$
		↓
		$H(1s, {}^2S) + e(p\text{-wave})$
$O_2^-(1\pi_g^1\ 3s\ \sigma_g^2, {}^2\pi_g)$[c]	→	$O_2(1\pi_g^2, {}^3\Sigma_g^+) + e$ (p wave)
$Na^-(3p^2, {}^3P^e) \rightarrow Na^-(3s3p, {}^3P^o) + h\nu \rightarrow$		$Na(3s, {}^2S) + e(p\text{-wave})$[d]

a) The electron is ejected with 19.4 eV of kinetic energy. The width of the resonance is 0.008 eV ($\tau \sim 5 \times 10^{-13}$ s) (Ref. 25).

b) This resonance lies ~ 0.01 eV below the 2p state of H and has a radiative decay rate to the $^3P^o$ state of $2.5 \times 10^6\ s^{-1}$. The $^3P^o$ state then decays via a Feshbach mechanism to H(1s) and e(p) at a rate of $6 \times 10^8\ s^{-1}$ (Ref. 26).

c) At 8.04 eV above the ground state of O_2, this resonance is thought to involve two electrons in a Rydberg-like $3s\sigma_g$ orbital bound to essentially an O_2^+ core (Ref. 27).

d) As explained in the text, the decay of $Na^-(3s3p, {}^3P^o)$ is not a Feshbach decay. This example is listed in this Table only to demonstrate that its seeming similarity to the above H^- case is deceiving. The $^3P^e$ state of Na^- lies 0.06 eV below the ^3P state of Na (Ref. 28).

The chemical importance of electronic Feshbach resonances derives from essentially the same effects as were given earlier for shape resonances. They allow either free electrons or electron density from a collision partner to give energy to the internal (vibrational, rotational, or electronic) degrees of freedom of the target.

Heavy Particle Shape Resonances. The van der Waals attraction between two Ar atoms is shown in Figure 3. It supports eight bound vibrational states if the diatom's rotational quantum number j is zero. For j = 30, only two vibrational states are bound. The angular momentum barrier arising from the $j(j+1)\hbar^2/2\mu r^2$ factor in the Ar_2 rotational kinetic energy gives rise to an effective radial potential (see Figure 3) which for j = 30 supports only two bound states and one metastable orbiting resonance state. Lower j values give rise to more bound states and more shape resonance states. The lifetimes of these states depend upon the height and thickness of the barrier, which depend upon j and the reduced mass and actually range (30) from 10^{-11} s to 10^{10} s.

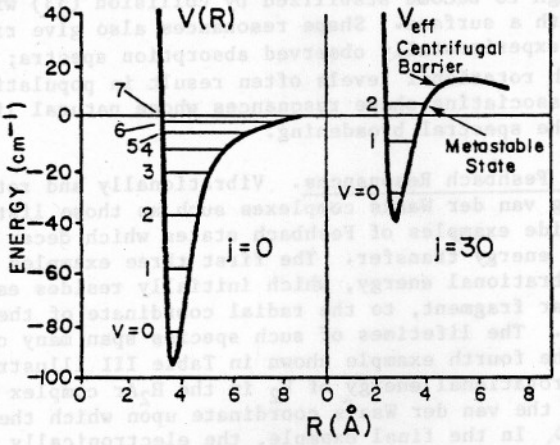

Figure 3: Intermolecular potential for Ar_2. On the left is the potential curve for non-rotating (j=0)Ar_2. On the right is the effective potential for rotating (j=30)Ar_2.

One can, of course, have orbiting resonances for larger molecules and for molecules in which chemical bonds (rather than van der Waals interactions) are operative. For example, H_2 (v = 0, j = 38) undergoes rotational predissociation to produce two H atoms. This metastable shape resonance state has a Heisenberg width (31) of 90 cm^{-1}; the v = 0, j = 37 state of H_2 decays with a width of 6 cm^{-1} and the v = 14, j = 4 state does so with $\Gamma \sim 0.007$ cm^{-1} (even though the v = 14, j = 4 state has far more total energy than the v = 0, j = 38 one).

Orbiting resonances are very important in chemistry. They have observable effects on the transport properties of dense gases and liquids (32), and they are thought to provide a mechanism for atom-atom recombination to occur via metastable shape resonances which live long enough to become stabilized by collision (33) with another molecule or with a surface. Shape resonances also give rise to broadening in experimentally observed absorption spectra; transitions into high rotational levels often result in populating rotationally predissociating shape resonances whose natural lifetime is reflected in the spectral broadening.

Heavy-Particle Feshbach Resonances. Vibrationally and rotationally predissociating van der Waals complexes such as those listed in Table III provide examples of Feshbach states which decay via intramolecular energy transfer. The first three examples involve transfer of vibrational energy, which initially resides essentially in one molecular fragment, to the radial coordinate of the weak van der Waals bond. The lifetimes of such species span many orders of magnitudes. The fourth example shown in Table III illustrates a case in which rotational energy of H_2 in the H_2Ar complex is transferred to the van der Waals coordinate upon which the system can dissociate. In the final example, the electronically excited HCN can, if it is prepared with excess energy in its bending vibrational mode (ν_2), undergo CH bond rupture if the excess bending energy transfers to the CH stretching mode (ν_1). The coupling between ν_2 and ν_1 is caused by strong off-diagonal curvature of the HCN molecule's potential energy surface between the bending and CH stretching coordinates, so the strength of this strong off-diagonal curvature determines the decay rate of C^1A' HCN.

The chemical importance of heavy-particle Feshbach resonances cannot be overstated. They are present in unimolecular rearrangements, both thermal ones and those which occur in organic photochemical reactions, in mass spectroscopic ion fragmentations, and in bimolecular collisions which proceed through long-lived intermediates.

A Novel Class of Target-Excited Resonance

Experiments have recently been carried out (1,3) in which polyatomic molecular anions trapped in an essentially collisionless ion cyclotron resonance cell are vibrationally excited using an infrared laser laser of 0.1-6 J/cm^2 fluence and $\sim$ 1000 cm^{-1} energy. Electron ejection from the anions is observed to occur at rates which are fluence dependent. The mechanism of this ejection is the subject of these remarks.

Table III. Heavy-Particle Feshbach Resonance Examples

Metastable Species		Decay Products
$I_2(B\ ^3\Pi,v)He$	→	$I_2(B\ ^3\Pi,v') + He$ [a]
$(C\ell_2)_2$	→	$2C\ell_2$ [b]
$NO_2(^2B)He$	→	$NO_2(^2B) + He$ [c]
$H_2(j,v)Ar$	→	$H_2(j',v) + Ar$ [d]
$HCN(C\ ^1A',\nu_1\nu_2\nu_3)$	→	$CN(B\ ^2\Sigma) + H$ [e]

a) A very strong propensity is observed for the v' = v - 1 channel. The rate of decay is 4.5 x 10^9 s^{-1} for v = 12 and increases to 2.6 x 10^{10} s^{-1} for v = 26 (Refs. 35,36).

b) The vibrationally excited $(C\ell_2)_2$ requires ~ 10^{-4} s to decay. This time is 10^8-10^9 times the vibrational period of the $C\ell_2$ moiety (Ref. 37).

c) The observed lifetime for the vibrationally hot ^2B state of NO_2 to eject the van der Waals bound He atom is 10^{-11} s (Ref. 38).

d) The rotationally hot H_2 moiety in H_2Ar decays via transfer of rotational energy to H_2...Ar relative motion with a width of ~ 10^{-3} cm^{-1} for j = 2 and 4 x 10^{-4} cm^{-1} for j = 4 (Refs. 39,40).

e) The bent excited state of HCN, when photochemically prepared from the X $^1\Sigma^+$ ground state, requires transfer from the bending (ν_2) motion to the CH stretching motion (ν_1) before dissociation can occur (Refs. 41,42).

Laser pulses of 3 μs duration and a typical fluence of 1.0 J/cm^2 and infrared absorption cross sections of 10^{-18}-10^{-20} cm^2 yield photon absorption rates of 10^5-10^7 photons/s, which are much slower than the rate of intramolecular vibrational energy redistribution in systems such as benzyl anion. Hence, the anions are excited in a sequential process in which the vibrational energy is redistributed before the next photon is absorbed. This means that such experiments cannot determine in which vibrational mode(s) the energy resides.

It has also been demonstrated (3), by studying the competition between electron loss and a unimolecular decomposition of known activation energy, that sequential infrared absorption continues to occur even after the anion has achieved enough total internal energy to reach its electron detachment threshold. This implies that, near threshold, electron ejection must not be occuring faster than the 10^5-10^7 s^{-1} photon absorption rate. These experiments do not, however, allow one to conclude with much certainty how far above

threshold photon absorption continues to occur; clearly, once the electron loss rate exceeds the absorption rate the anion will no longer absorb.

The above experiments are hampered by lack of knowledge of the total energy content and internal energy distribution of the anions. This interpretation would be helped by order of magnitude estimates of the rate of electron ejection as a function of energy above threshold. The author's group recently undertook (4) an *ab initio* simulation of such ejection rates for two prototype anions (OH^- and LiH^-) which are viewed as limiting cases of slow (OH^-) and rapid (LiH^-) vibration induced electron ejection. Diatomic anions were chosen to obviate questions about where (i.e., in what vibrational mode) the internal energy is residing. OH^- is an ideal candidate for slow electron loss because the energy of its 1π active orbital is only weakly dependent upon bond length and because its detachment threshold is large (1.82 eV). In contrast, the 3σ active orbital of LiH^-, which consists primarily of a nonbonding 2s-2pσ hybrid localized on the Li center and directed away from the H center, is quite strongly affected by movement of the very polar (Li^+H^-) bond. As a result, the detachment energy of LiH^- varies substantially with bond length; even at the equilibrium bond length it is only 0.3 eV.

For neither LiH^- nor OH^- do the anion and neutral Born-Oppenheimer potential energy curves cross. Such is also thought to be the case for the energy surfaces of the polyatomic anions studied in the experiments of Refs. (1) and (3) and for the curves of ($B\ ^2\Sigma_u^+$) C_2^- and ($X\ ^1\Sigma_g^+$ or a $^3\Pi_u$) C_2 where Lineberger (43) has observed ($B\ ^2\Sigma_u^+$) C_2^- to be metastable with respect to electron ejection. Hence the electron loss mechanism does *not* involve the anion sampling, through its vibrational motion, geometries where electronic shape or Feshbach resonances or direct detachment occurs. It requires coupling between electronic and vibrational motion and can be viewed as a radiationless transition between the two components of the metastable state (the vibrationally excited anion and the vibrationally cooler neutral with an outgoing electron) induced by the nonadiabatic coupling terms which the Born-Oppenheimer Hamiltonian neglects. In this sense, such metastable states can be viewed as target-excited states. They are analogous to vibrationally excited Rydberg states which undergo autoionization (44).

It was found in Ref. (4) that the lifetimes for electron ejection ranged from 10^{-9} to 10^{-10} s for LiH^- in vibrational levels between v = 3 and v = 10 and from 10^{-5} to 10^{-6} s for OH^- from v = 5 to v = 11. The ejection rates did not increase strongly with increasing vibrational energy above threshold. In all cases, the anions were found to decay preferentially to the energetically closest vibrational state of the neutral; the branching ratios for decay into various neutral vibrational levels correlated well with ion-neutral Franck-Condon-like factors.

This range of lifetimes (10^{-9}-10^{-10} to 10^{-5}-10^{-6} s) for prototype fast and slow electron ejectors is entirely consistent with the estimates made in Refs. (1), (3) and (43). The weak dependence of these rates on the energy above threshold indicates that many polyatomic anions (i.e., those for which the ejection rate

near threshold is not faster than the photon absorption rate) continue to absorb infrared photons far above their detachment thresholds. This information, when combined with the observation of a propensity to decay to the closest vibrational level of the neutral, suggests that vibrationally hot neutrals can be expected to be produced in such infrared pumping experiments. When considering the reverse reaction, the attachment of an electron to a molecular target to produce a vibrationally hot anion, the rate of electron ejection as studied here can be combined with estimates of the equilibrium constant for

$$e + A(v) \rightleftarrows A^-(v')$$

to estimate the rate constant for the attachment step. Benson has actually done so (45) in a recent study of SF_6^-.

Acknowledgments

Acknowledgment is made to the National Science Foundation (Grant #8206845), as well as to the Donors of the Petroleum Research Fund, administered by the American Chemical Society (PRF 14446-AC6), for their support.

Literature Cited

1. Meyer, F. K.; Jasinski, J. M.; Rosenfeld, R. N.; Brauman, J. I. J. Am. Chem. Soc. 1982, 104, 663; Rosenfeld, R. N.; Jasinski, J. M.; Brauman, J. I. J. Chem. Phys. 1979, 71, 1030; Wight, C. A.; Beauchamp, J. L. J. Am. Chem. Soc. 1982, 103, 6501.
2. Simons, J. J. Am. Chem. Soc. 1981, 103, 3971.
3. Foster, R. F.; Tumas, W.; Brauman, J. I. J. Chem. Phys. 1983, 79, 4644.
4. Acharya, P. K.; Kendall, R. A.; Simons, J. J. Am. Chem. Soc. 1984, 00, 0000.
5. Taylor, H. S.; Nazaroff, G. V.; Golebiewski, A. J. Chem. Phys. 1966 45, 2872.
6. Bardsley, J.N.: Herzenberg, A.; Mandl, F. Proc. Phys. Soc. London 1966, 89, 321.
7. Eliezer, I.; Taylor, H.S.; Williams, J. K. J. Chem. Phys. 1967, 47, 2165.
8. Schulz, G. J. Phys. Rev. 1964, 135, A988; 1964, 136, A650.
9. Trajmar, S.; Truhlar, D. G.; Rice, J. K.; Kuppermann, A. J. Chem. Phys. 1970, 52, 4516.
10. Schulz, G. J.; Asundi, R. K. Phys. Rev. 1967, 158, 25.
11. Herzenberg, A.; Mandl, F. Proc. Roy. Soc. 1962, A270, 48.
12. Schulz, G. J.; Koons, H. C. J. Chem. Phys. 1966, 44, 1297.
13. Herzenberg, A. J. Phys. 1968, B1, 548.
14. Birtwistle, D. T.; Herzenberg, A. J. Phys. 1971, B4, 53.
15. Burrow, P. D.; Michejda, J. A.; and Comer, J. J. Phys. 1976, B9, 3255.
16. Hazi, A. V. J. Phys. 1978, B11, L259.
17. Donnelly, R. A. J. Chem. Phys. 1982, 76, 5914.
18. Mishra, M.; Kurtz, H.; Goscinski, O.; Ohrn, Y. J. Chem. Phys. 1983, 79, 1896.

19. Novick, S. E.; Jones, P. L.; Mulloney, T. J.; Lineberger, W. C. J. Chem. Phys. 1979, 70, 2210.
20. Collins, L.A.; Norcross, D. W. Phys. Rev. Lett. 1977, 38, 1208.
21. Blais, N. C.; Truhlar D. G. J. Chem. Phys. 1983, 79, 1334; McGuire, P.; and Bellum, J. C. J. Chem. Phys. 1979, 71, 1975.
22. Hertel, I. V.; Hofmann, H.; Rost, K. A. Chem. Phys. Lett. 1977, 47,163.
23. Breckenridge, W. H.; Umemoto, H. J. Chem. Phys. 1981, 75, 698.
24. Jordan, K. D.; Burrow, P. D. Acc. Chem. Res. 1978, 11, 341.
25. Sanche, L.; Schulz, G. J. Phys. Rev. 1972, A5, 1672.
26. Drake, G. W. F. Astrophys. J. 1973, 184, 145.
27. Sanche, L.; Schulz, G. J. Phys. Rev. 1972, A6, 69.
28. Norcross, D. W. Phys. Rev. Lett. 1974, 32, 192.
29. Moiseyev, N.; Weinhold, F. Phys. Rev. 1979, A20, 27.
30. Ewing, G. E. Can. J. Phys. 1976, 54, 487; Acc. Chem. Res. 1975, 8, 185.
31. Leroy, R. J. Ph.D. Thesis, University of Wisconsin, 123, 1971.
32. Hirschfelder, J. O.; Curtiss, F. F.; Bird, R. B. Molecular Theory of Gases and Liquids 1967, J. Wiley and Sons, N.Y. See p. 555.
33. Roberts, R. E. Ph.D. Thesis, University of Wisconsin, 1968.
34. Herzberg, G. Molecular Spectra and Molecular Structure I. Spectra of Diatomic Molecules 1950, Van Nostrand Reinhold, N.Y. See pp. 425-430.
35. Johnson, K. E.; Wharton, L.; Levy, D. H. J. Chem. Phys. 1978, 69, 2719.
36. Beswick, J. A.; Jortner, J. Adv. Chem. Phys. 1981, 47, 363.
37. Dixon, D. A.; Herschbach, D. R. Ber. Bunsen Ges. Phys. Chem. 1977, 81, 145.
38. Smalley, R.; Wharton, L.; Levy, D. H. J. Chem. Phys. 1977, 66, 2750.
39. Leroy, R. J.; Carley, J. S. Adv. Chem. Phys. 1980, 42, 353.
40. Beswick, J. A.; Requena, A. J. Chem. Phys. 1980, 72, 3018.
41. Chuljian, D. T.; Ozment, J.; Simons, J. J. Chem Phys. 1984, 80, 176; Inter. J. Quantum Chem. 1982, S16, 435.
42. Macpherson, M. T.; Simons, J. P. J. Chem. Soc. Faraday Trans. II 1978, 74, 1965.
43. Jones, P. L.; Mead, R. D.; Kohler, B. E.; Rosner, S. D.; Lineberger, W. C. J. Chem. Phys. 1980, 73, 4419.
44. Berry, R. S. J. Chem. Phys. 1966, 45, 1228.
45. Heneghan, S. P.; Benson, S. W. Inter. J. Chem. Kin. 1983, 15, 109.

RECEIVED June 11, 1984